

# Unified Face Matching and Physical-Digital Spoofing Attack Detection

Arun Kunwar and Ajita Rattani  
Dept. of Computer Science and Engineering,  
University of North Texas at Denton, USA

arunkunwar@my.unt.edu, ajita.rattani@unt.edu

## Abstract

*Face recognition technology has dramatically transformed the landscape of security, surveillance, and authentication systems, offering a user-friendly and non-invasive biometric solution. However, despite its significant advantages, face recognition systems face increasing threats from physical and digital spoofing attacks. Current research typically treats face recognition and attack detection as distinct classification challenges. This approach necessitates the implementation of separate models for each task, leading to considerable computational complexity, particularly on devices with limited resources. Such inefficiencies can stifle scalability and hinder performance. In response to these challenges, this paper introduces an innovative unified model designed for face recognition and detection of physical and digital attacks. By leveraging the advanced Swin Transformer backbone and incorporating HiLo attention in a convolutional neural network framework, we address unified face recognition and spoof attack detection more effectively. Moreover, we introduce augmentation techniques that replicate the traits of physical and digital spoofing cues, significantly enhancing our model robustness. Through comprehensive experimental evaluation across various datasets, we showcase the effectiveness of our model in unified face recognition and spoof detection. Additionally, we confirm its resilience against unseen physical and digital spoofing attacks, underscoring its potential for real-world applications.*

## 1. Introduction

Facial recognition has transformed security and convenience across various sectors, including smartphone unlocking, law enforcement, surveillance, retail personalization, and healthcare, highlighting its wide-reaching impact and transformative potential [21, 39]. It typically operates through a three-stage pipeline: face detection, feature extraction, and face matching. The detection stage identifies facial regions in an image or video, while the feature ex-

traction stage encodes distinctive facial attributes into high-dimensional vectors using deep learning architectures like Convolutional neural networks (CNNs) or Transformers. In the matching stage, these feature vectors are compared using distance metrics such as cosine similarity or euclidean distance to verify or recognize identities [43, 53].

The transformer architecture, with its ability to model global dependencies and spatial relationships through self-attention mechanisms, has obtained state-of-the-art results in image classification, object detection, and segmentation tasks, exceeding traditional CNN-based approaches [41]. In the context of face recognition, Transformers, such as the Swin Transformer [34], resulted in the extraction of more discriminative facial features, utilizing self-attention mechanisms, positional encodings, and hierarchical structures to integrate both local and global features. Thus, achieving state-of-the-art performance in face recognition by addressing challenges such as pose variations, lighting changes, and occlusion [41].

However, facial recognition systems<sup>1</sup> are increasingly vulnerable to adversarial attacks. Driven by objectives such as financial gain or personal disputes, malicious users often exploit these vulnerabilities by presenting pre-captured or digitally manipulated photos or videos or by using masks and accessories to circumvent the system. This highlights the critical importance of implementing robust security measures to detect and prevent such threats. Facial attacks can be broadly categorized into two main categories: *physical* and *digital* spoofing attacks. Physical spoofing attacks involve real-world manipulations like print [28, 61, 62], replay [26, 27], and 3D mask attacks [14, 22, 29, 30]. Digital attacks include any kind of digital manipulation to the images such as adding adversarial noise perturbation, image morphing and deepfakes. Digital spoofing attacks based on facial manipulation based deepfakes depict human subjects with altered identities (identity swap) [44], attributes, or malicious actions and expressions (face reenactment) in a given image or a video [8, 18]. Within the *scope* of this

<sup>1</sup>The term face recognition and face matching have been used interchangeably in this paper.

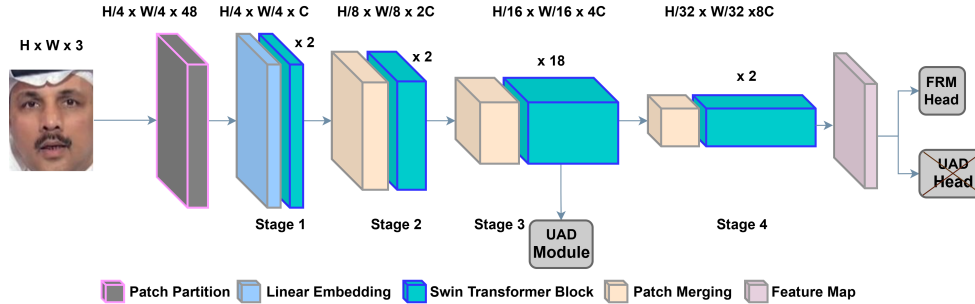


Figure 1. Unified architecture illustrating the integration of the FRM head at the output of the Swin Transformer backbone for face recognition and the UAD module appended at the intermediate layers of Stage 3, specifically for joint physical-digital attack detection. The crossed-out UAD head at the final stage highlights the ineffectiveness of positioning the UAD head at the output of the Swin Transformer backbone. This is because the final layer classification features from the Swin Transformer backbone are not optimal for joint physical and digital attack detection.

study, only digital attacks involving facial manipulations are considered. Further, they also include attacks based on adversarial noise perturbations in images to mislead the system [7, 20].

Extensive research has been conducted on facial recognition [21, 53, 63], physical [26, 28, 61, 62], and digital spoofing attack detection [40] as distinct classification tasks, each demonstrating significant performance improvement. However, deploying separate models for facial recognition, and physical and digital attack detection introduces substantial computational overhead, particularly on resource-constrained devices, thereby limiting efficiency and scalability. This challenge underscores the need for an integrated (unified) framework that can concurrently address face recognition, with joint physical-digital spoofing attack detection, while ensuring optimal performance, resource utilization, and scalability, paving the way for more efficient and adaptable solutions for real-world applications.

Few studies [2, 23, 54] have explored the use of Transformers for unified facial recognition and physical spoof detection. Mostly, a dual-head Transformer architecture that shares a common backbone and adds two classification heads at the end for joint recognition and physical attack detection, has been used for the unified task [2]. However, face recognition depends on high-level, identity-specific features, while physical or digital attack detection relies on fine-grained, local details such as texture and noise [23, 54]. Dual-head architectures, which share a common feature space, often underperform due to the mismatch in feature requirements for recognition and spoof classification tasks [2]. Recent research addresses this limitation by using intermediate features from the Transformer for physical attack detection and identity-specific features from the last layers for face recognition [2].

With the availability of unified attack datasets comprising both physical and digital facial attacks for the same

identities, recently unified physical and digital attack detection methods are proposed using optimized data augmentation [15] and balanced loss functions [60], and the joint use of CLIP and a Multi-Layer Perceptron (MLP) [25]. However, these unified attack detection studies *do not* include facial recognition.

This paper proposes a unified model for face recognition and joint detection of physical and digital spoof attacks for the *first* time. To achieve this, we leverage the Swin Transformer architecture [34] as the backbone along with HiLo attention [37] and a CNN-based classification in local blocks of the Swin Transformer for joint detection of physical and digital spoofing attacks (as a part of the unified attack detection (UAD) module). The global classification head is appended at the end of the Transformer backbone for face representation and matching (FRM). HiLo attention is used for joint physical-digital attack detection to effectively capture high-frequency details, such as subtle artifacts and fine-grained textures, along with low-frequency information that preserves the broader contextual structure of the image or video [59]. This combination of localized detailed analysis and global contextual understanding strengthens the model’s capability to accurately and reliably detect both kind of spoofing attacks. By separating attention heads into groups based on high-frequency and low-frequency patterns, HiLo attention enables the model to detect a wide range of attacks, from localized manipulations to global distortions. Data enhancement simulating physical and digital cues is added to further facilitate joint physical-digital attack detection. Figure 1 shows the overall architecture of the proposed unified model for face representation and matching (FRM) and joint physical-digital attack detection (UAD module).

**Contributions:** In summary, the main **contributions** of this paper are summarized as follows:

- Developing a unified model capable of performing both face recognition and joint physical and digital attack detection using the Swin Transformer as a backbone.
- Using HiLo attention along with CNN architecture appended to intermediate transformer blocks (UAD module) to capture both high-frequency and low-frequency image features required for joint physical and digital facial attack detection.
- Adding data augmentations simulating physical and digital attack cues resulting in UAD module efficacy in detecting both physical-digital as well as unknown attacks.
- Extensive evaluation of the unified model’s capability in face recognition, physical, and digital facial spoof attack using diverse datasets and across unknown attack detection scenario.

## 2. Related Work

### 2.1. Face Representation and Matching

Face recognition systems have significantly advanced, evolving from traditional approaches such as holistic methods [4] and handcrafted features [6, 31] to modern deep learning-based models. Traditional methods struggled to manage large intra-class variations and inter-class similarity, a limitation effectively addressed by deep-learning based methods [38, 46, 49, 51]. Notable CNN-based systems such as DeepFace [19], DeepID [56], and FaceNet [1] have demonstrated notable performance in face recognition.

Recent studies demonstrated the efficacy of Vision Transformers for face recognition. For instance, [63] utilized Vision Transformer (ViT) models for face matching, demonstrating state-of-the-art performance on large-scale datasets. [42] demonstrate the effectiveness of the Swin Transformer in face recognition, facial expression, and age estimation tasks. Similarly, [48] proposed fViT, a Vision Transformer baseline that surpasses state-of-the-art face recognition methods. They also introduced part fViT, a part-based approach for facial landmarks and patch extraction, obtaining state-of-the-art accuracy on multiple facial recognition benchmarks. [50] proposed a cross-attribute-guided Transformer framework combined with self-attention distillation to enhance low-quality face recognition.

### 2.2. Unified Models

The study in [2] proposed a dual-head approach for unified face recognition and physical attack detection that incorporates separate classification heads for each of these tasks, utilizing shared features from a common Vision Transformer (ViT) backbone. However, the performance

of this method was suboptimal due to the differing feature requirements of the two tasks. To address this issue, the authors of [2] introduced a unified framework that leverages local features from the intermediate layers of the ViT for detecting physical attacks while utilizing the class token from the final layer of the ViT for face recognition. Similarly, [47] proposed a unified approach for both face recognition and physical attack detection by combining the Fisherface algorithm with local binary pattern histograms (LBPH) and deep belief networks. In this method, Fisherface is used to recognize faces by reducing the dimensionality in the facial feature space through LBPH, while a deep belief network with a Restricted Boltzmann Machine serves as a classifier for detecting deepfake attacks. [32] combines Kinect sensors with FaceNet to enhance liveness detection and identity authentication. These aforementioned models perform unified face matching and physical attack detection. In *contrast*, our proposed unified model performs face matching along with joint physical-digital spoof detection.

## 3. Proposed Method

The primary objective of this work is to develop a multi-task model capable of obtaining optimal performance in both face representation and matching (FRM) and unified attack detection (UAD) (both physical and digital spoofing attacks). To accomplish this, we use the Swin Transformer as the backbone and evaluate a hybrid multi-task architecture. The FRM head is placed at the end of the backbone to leverage deep features critical for face recognition (see Figure 1). For the UAD module, HiLo attention with a CNN is used to leverage the rich local features extracted from the intermediate layers of the Swin Transformer. Further, the training data is augmented using Simulated Physical Spoofing Clues (SPSC) and Simulated Digital Spoofing Clues (SDSC) methods (detailed in section 3.3), enabling effective training of UAD module for joint physical-digital spoofing attack detection.

### 3.1. Swin Backbone

The base Swin Transformer backbone [34] has four hierarchical stages that reduce spatial dimensions and increase feature depth via patch merging. Each stage includes Swin Transformer blocks with Shifted Window Multi-Head Self-Attention (SW-MHSA), a Feedforward Network (FFN), Layer Normalization (LN), and residual connections. The input image  $x \in \mathbb{R}^{H \times W \times C}$  (where  $H$ ,  $W$ , and  $C$  represent the height, width, and number of channels of the image, respectively) is first divided into non-overlapping patches of size  $4 \times 4$  using a patch partitioning layer, resulting in an initial sequence of patch embeddings  $Z_0 \in \mathbb{R}^{\frac{H}{4} \times \frac{W}{4} \times C'}$ , where  $C' = 128$  represents the embedding dimension of each patch for the base model. This initial patch embedding forms the input to the hierarchical architecture, with each

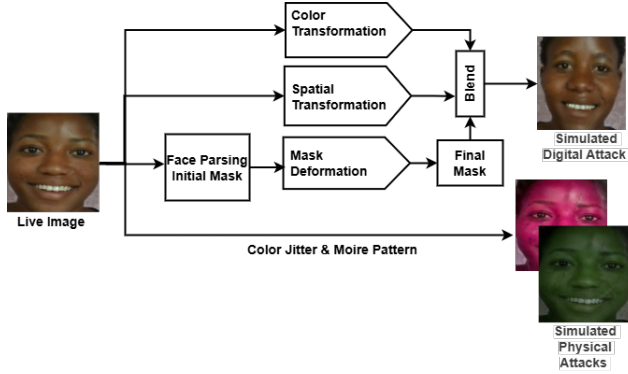


Figure 2. Illustration of the data augmentation process for a live face sample into physical and digital attack cues using SPSC and SDSC augmentation techniques.

stage processing and refining the features for higher-level representations.

The SW-MHSA mechanism processes patches within local windows of size  $M \times M$ , where  $M = 7$  in the base Swin Transformer, reducing computational complexity compared to global attention. To enable cross-window interaction, the shifted window approach alternates between regular and shifted windows across layers. Let  $Z^\ell = [z_1^\ell, z_2^\ell, \dots, z_n^\ell] \in \mathbb{R}^{n \times C'}$  denote the output of the  $\ell$ -th Swin Transformer block, where  $n$  is the number of patch tokens and  $C'$  is the embedding dimension. The Swin Transformer processes the input image hierarchically through multiple stages, with patch merging layers at each stage reducing the spatial size of the token map while increasing the embedding dimensions. The hierarchical structure produces a compact representation  $Z_L \in \mathbb{R}^{N \times D}$  after the final stage, where  $N$  represents the number of tokens in the final stage, determined by the resolution of the input and the down-sampling factor and  $D$  is the dimensionality of the output features.

Typically, the final feature map output of the last stage can be pooled or directly used as a latent representation for downstream tasks, allowing the Swin Transformer backbone to act as an encoder  $E_\omega$ , mapping an input image  $x$  to its latent feature representation  $Z_L$ , i.e.,  $Z_L = E_\omega(x)$ . This hierarchical architecture allows the Swin Transformer to effectively capture local and global features for classification and detection tasks.

### 3.2. Unified Attack Detection Module

The Unified Attack Detection (UAD) module combines HiLo attention with a lightweight convolutional network (CNN) to enhance spoofing attack detection by leveraging intermediate features from the Swin Transformer backbone, as these shallow features effectively capture local patterns essential for joint physical-digital spoofing attack detection. The HiLo attention module [37] processes these features by

separating attention into high-frequency (Hi-Fi) and low-frequency (Lo-Fi) components, extracting local details and global patterns separately. The Hi-Fi path, with 4 attention heads, uses local window self-attention over  $2 \times 2$  windows to capture fine-grained details efficiently, while the Lo-Fi path applies average pooling within each window to extract low-frequency signals for modeling relationships with query positions. Features from both paths are concatenated and processed through the CNN, which comprises two convolutional layers, max-pooling, and fully connected layers. The final output, predicting live vs. spoofed faces, is obtained via a sigmoid activation function, enabling joint physical-digital attack detection, as shown in Figure 3.

### 3.3. Simulating Spoofing Cue Augmentation

The Simulated Physical Spoofing Clues (SPSC) augmentation [17] enhances spoof detection by simulating physical attack characteristics through ColorJitter and moiré pattern augmentation (Figure 2). ColorJitter replicates color distortions in print attacks by adjusting brightness, contrast, saturation, and hue, while moiré pattern augmentation mimics artifacts from replay attacks through pixel remapping and polar transformations. This strategy diversifies the dataset and improves model robustness against spoofing.

The Simulated Digital Spoofing Clues (SDSC) augmentation technique [17] replicates digital forgery artifacts, such as face swapping, through a three-step process. First, it duplicates the original image to create pseudo-source and target images, augmented with color (e.g., hue, brightness) and spatial transformations (e.g., resize, translate), producing misaligned boundaries (see Figure 2). Second, a face mask is generated using a face parsing algorithm and deformed with spatial transformations, elastic distortions, and blurring. Finally, the pseudo-source and target images are blended using the deformed face mask to create a synthetic forgery, enriching the dataset with realistic artifacts to enhance the model’s ability to detect such attacks.

### 3.4. Our Unified Architecture: FRM and UAD

The proposed unified architecture employs a Swin Transformer backbone to perform both FRM and UAD tasks, as depicted in Figure 1. Initially, the backbone is trained for FRM, utilizing global and deep features ( $7 \times 7 \times 1024$ ) extracted from its final stage. This is facilitated through appending an MLP-based FRM head at the end of the backbone for face recognition. This head utilizes the output features of the Swin Transformer and applies L2 normalization to the feature embeddings, mapping them onto a unit hypersphere. This hyperspherical normalization ensures consistent embedding magnitudes, allowing the ArcFace loss function (see equation 1) to effectively enhance class separability and ensure robust performance.

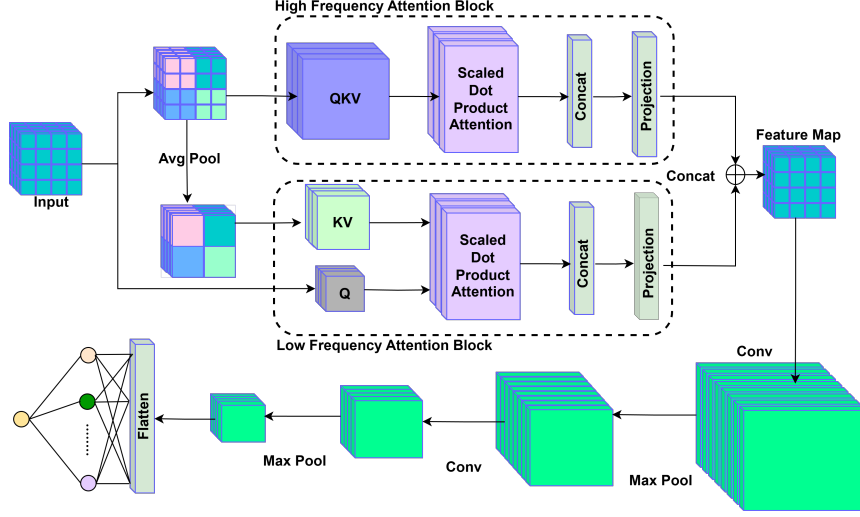


Figure 3. UAD module leveraging Stage 3 intermediate features along with HiLo attention and a cascaded CNN for joint physical-digital attack detection. High-frequency and low-frequency blocks use an attention module defined as a scaled dot-product function, where query, key, and value matrices are denoted as Q, K, and V, respectively.

Given  $N_{id}$  training samples and  $C$  unique identities in the dataset, the loss function is defined as

$$\mathcal{L}_{FRM} = -\frac{1}{N_{id}} \sum_{i=1}^{N_{id}} \log \frac{e^{s \cos \tilde{\theta}_{y_i^{id}}}}{e^{s \cos \tilde{\theta}_{y_i^{id}}} + \sum_{j=1, j \neq y_i^{id}}^C e^{s \cos \theta_j}}, \quad (1)$$

where  $\cos \tilde{\theta}_{y_i^{id}} = \cos(\theta_{y_i^{id}} + m)$ . Here,  $\cos \theta_r$  represents the cosine similarity between the normalized feature vector  $v$  and the weight vector  $W_r$ , with  $\|W_r\|$  and  $\|v\|$  denoting their  $L_2$  norms. The parameters  $s$  (scale) and  $m$  (angular margin) control the strength of the feature scaling and margin, respectively. By modifying the decision boundaries in the angular space, the ArcFace loss significantly improves the network’s ability to distinguish between different identities, making it ideal for face recognition tasks [13].

After FRM training, the backbone is frozen, and the UAD head is appended at the intermediate layer of Stage 3 ( $14 \times 14 \times 512$ ), where shallow features effectively capture local and attack-specific patterns. This stage is preferred because it contains 18 attention blocks, significantly more than the 2 blocks in other stages. These multiple blocks represent varying levels of feature abstraction, providing a broader range of feature representations to test and determine the optimal level for the detection task. The UAD module also utilizes a HiLo Attention module to extract both high- and low-frequency features from the intermediate outputs of Stage 3, followed by a lightweight convolutional network for binary classification, trained using Bi-

nary Cross-Entropy loss (see equation 2).

$$L_{SD} = -\frac{1}{N_s} \sum_{i=1}^{N_s} [y_i^s \log(\hat{y}_i^s) + (1 - y_i^s) \log(1 - \hat{y}_i^s)], \quad (2)$$

where  $N_s$  is the number of attack samples (physical and digital),  $y_i^s \in \{0, 1\}$  is the ground truth label for sample  $i$ , and  $\hat{y}_i^s$  is the predicted probability for the same sample. Here, the labels 0 and 1 represent the spoof attack (both digital and physical) and bonafide face image, respectively. Training of UAD for attack detection is enhanced using SPSC and SDSC augmentations, simulating print, replay, and digital attacks.

Additional training configurations are also explored, where the UAD head is appended at the final layer of the backbone and trained with and without freezing the backbone, to evaluate the performance trade-off for unified FRM and UAD tasks as shown in Figure 1. This comprehensive training strategy allows for assessing the effectiveness of intermediate and final layer features for multi-tasking performance.

## 4. Experimental Implementations

### 4.1. Datasets

The CASIA-WebFace dataset [57] is utilized for training the face recognition model. The FaceForensics++ [45] and CelebDF [24] datasets are utilized for benchmarking the accuracy of the face recognition model across datasets. Similarly, the UniAttack dataset [15], augmented using the SPSC and SDSC methods, is used to train the UAD module. FaceForensics++(FF++), SIW-Mv2 [16] and MSU Mobile

Face Spoofing Database (MSU-MFSD) [55] datasets are used for the evaluation of the UAD module. Further, SiW-Mv2 and Diverse Fake Face Dataset (DFFD) [11] dataset are used to test the model performance on unknown physical and digital attacks, respectively. Face crops from facial images extracted from the videos were obtained using the Multi-task Cascaded Convolutional Neural Network (MTCNN) [60], a deep learning framework designed for efficient face detection and alignment. The cropped facial images were resized to  $224 \times 224$  pixels for further processing.

To evaluate the accuracy of the FRM trained on the CASIA-WebFace dataset, 10,000 image pairs with matching identities and 10,000 pairs with non-matching identities were selected from the live image sets of FaceForensics++ and CelebDF. The Swin Transformer model was employed for feature extraction, and cosine similarity was used to measure the model’s performance. The UAD model was trained using the UniAttack dataset, augmented with SPSC and SDSC techniques. For cross-dataset evaluation, 20,000 live and 20,000 spoof images (FaceShift, FaceSwap, and Face2Face) were selected from FaceForensics++, 5,000 live and 5,000 spoof images (replay and print attacks) from the SiW-Mv2 dataset, and 175 live and 525 spoof images from the MSU-MFSD dataset.

The model’s performance against unknown attacks was evaluated using a variety of spoofing categories from the SiW-Mv2 and DFFD datasets. Physical spoof categories included Makeup Cosmetics, Makeup Impersonation, Makeup Obfuscation, Mannequin, Mask Half Mask, Mask Paper Mask, Mask Transparent Mask, as well as partial spoofs such as Partial Eye, Partial Funny Eye Glasses, Partial Mouth, and Partial Paper Glasses, along with Silicone masks. The DFFD dataset comprises of a rich variety of manipulations, including identity and expression swaps sourced from FaceForensics++, facial attribute edits using FaceAPP, and synthetic faces created with GANs like StyleGAN and PGGAN. It offers high-quality images that represent a broad spectrum of manipulations, from subtle attribute changes to fully synthetic faces.

## 4.2. Implementation Details

The Swin base model, pretrained on ImageNet-21K is used as the backbone. It consists of four stages with 2, 2, 18, and 2 transformer blocks in each stage, respectively. The model processes images by dividing them into patches and progressively reducing spatial dimensions while increasing feature depth across stages [34]. The FRM head includes a fully connected layer that projects the  $d$ -dimensional output of the Swin Transformer backbone into a 1024-dimensional face embedding. The feature embedding is normalized and ArcFace loss is applied with an angular margin to enforce inter-class separability and intra-class compactness,

ensuring highly discriminative features optimized for face recognition. This FRM head is fine-tuned on the CASIA-WebFace dataset using the ArcFace loss (scale  $s = 32$ , margin  $m = 0.5$ ) and optimized with the stochastic gradient descent (SGD) algorithm at a fixed learning rate of  $10^{-3}$ . Training is performed with a batch size of 64 using an early stopping mechanism to avoid overfitting.

The total size of our FRM system model, which combines the Swin Transformer backbone with 86.7M parameters and the ArcFace loss function with 10.8M parameters (for 10,572 classes), is 97.5M parameters.

Similarly, the UAD module comprising of an immediate HiLo attention block, followed by two convolutional layers (64 and 32 layers with  $3 \times 3$  kernel), a fully connected layer of size 128, and a sigmoid activation is appended to each intermediate block of Stage 3, as well as to the final layer, resulting in 19 independent classifiers (18 classifiers from Stage 3). For each UAD module training, the UniAttack dataset and its augmentations (SPSC and SDSC) are utilized. It is trained under two settings: with the Swin Transformer backbone frozen and unfrozen. All UAD modules are trained under identical hyperparameter settings for consistent comparison. The UAD model’s architecture is lightweight, comprising approximately 1.2 million parameters, facilitating efficient training and inference for joint spoofing attacks. Trained using binary cross-entropy loss, the classifiers’ parameters are optimized with SGD at a learning rate of  $10^{-3}$  using a batch size of 64 using an early stopping mechanism.

## 4.3. Evaluation Metrics

The FRM task is assessed by measuring face-matching accuracy, determined through face verification for fair comparison with [2]. The performance of the UAD classifier is evaluated using metrics such as Attack Presentation Classification Error Rate (APCER), Bona Fide Presentation Classification Error Rate (BPCER), and classification accuracy [15, 60]. Additionally, the Equal Error Rate (EER) is computed to provide a more precise and comprehensive evaluation of both the FRM and UAD tasks.

## 5. Results and Discussion

**FRM Evaluation.** Firstly, the Swin Transformer backbone pretrained on ImageNet-21K, combined with the FRM head, is fine-tuned on the CASIA-WebFace dataset and evaluated on FF++ and CelebDF datasets for face recognition tasks. Our model obtained 99.43% accuracy on FF++, surpassing the 98.96% reported in [2] and is at par with 99.53% across datasets in [13], also shown in Table 2.

The same model is fine-tuned for the UAD head appended at the end using the augmented UniAttack dataset and evaluated on the FF++ and CelebDF datasets for FRM

Training Scenario	FF++		Celeb DF	
	Acc (%)	EER (%)	Acc (%)	EER (%)
FRM Finetuned	<b>99.43</b>	<b>1.23</b>	<b>95.23</b>	<b>4.00</b>
UAD Finetuned	95.03	5.46	86.50	15.3

Table 1. Face matching accuracy on FF++ and CelebDF datasets: (Row 1) Swin Transformer model fine-tuned for FRM using CASIA-WebFace dataset and (Row 2) the same model further fine-tuned for UAD using augmented UniAttack dataset, tested for FRAM (face recognition performance).

Study	Model	Accuracy (%)
Deng et al. (2022) [13]	ResNet50	99.53
Al-Refai et al. (2023) [2]	ViT	98.96
<b>Ours (FRM Finetuned)</b>	<b>Swin-T</b>	<b>99.43</b>

Table 2. Performance of existing and our proposed model for FRM task.

Finetuned (UAD Head)	FF++		SiW		MSU-MFSD	
	Acc (%)	EER (%)	Acc (%)	EER (%)	Acc (%)	EER (%)
SWIN unfrozen	51.32	44.78	55.34	49.46	75.65	58.53
SWIN frozen	<b>74.67</b>	<b>26.92</b>	<b>63.45</b>	<b>38.47</b>	<b>75.54</b>	<b>51.17</b>

Table 3. Cross-dataset performance comparison for UAD head fine-tuned with and without freezing Swin transformer backbone. Training was performed on the augmented UniAttack dataset. Results include accuracy (Acc) and equal error rate (EER) for FF++ (Digital: Deepfakes, Face2face and Faceswap), SiW (Physical: Paper and Replay), and MSU-MFSD (Physical: Paper and Replay) datasets.

(Table 1). Results show that fine-tuning the Swin Transformer for UAD head reduces FRM accuracy, with a 4.4% drop on FF++ and 8.73% on CelebDF, highlighting the complimentary nature of features used for UAD and FRM tasks.

**UAD Evaluation.** UAD was evaluated under two scenarios. In the first scenario, the UAD head was appended to the end of the Swin transformer, and the model was fine-tuned with and without freezing the backbone. In both setups, the UAD performance remains suboptimal, indicating that the features extracted at deeper layers are not well-suited for UAD tasks as illustrated in Table 3. This is likely because deeper layers focus on high-level features, while UAD relies more on low-level features essential for effective attack detection.

In the second scenario, the Swin Transformer backbone was frozen, and UAD modules were appended at all intermediate blocks of Stage 3 of the Swin Transformer, with each UAD module trained independently. Performance was evaluated on FF++, SiW-Mv2, and MSU-MFSD datasets, trained using the augmented UniAttack dataset, as shown

Stage 3 Blocks	FF++		SiW-Mv2		MSU-MFSD	
	Acc (%)	EER (%)	Acc (%)	EER (%)	Acc (%)	EER (%)
0	95.4	5.2	67.4	33.5	75.3	30.6
1	96.5	4.4	69.7	32.3	74.7	30.3
2	96.1	4.1	74.0	29.3	76.7	32.7
3	97.0	3.9	76.6	25.2	77.1	28.4
4	96.6	4.3	81.5	19.7	75.0	23.5
<b>5</b>	<b>97.2</b>	<b>4.1</b>	<b>86.8</b>	<b>14.2</b>	<b>79.1</b>	<b>19.5</b>
6	96.3	4.1	82.3	20.6	75.8	31.3
7	95.1	5.3	83.4	20.2	76.9	29.1
8	95.2	5.8	81.8	21.1	81.4	22.7
9	93.3	7.6	77.2	23.4	78.0	22.4
10	91.9	9.1	78.3	23.4	76.4	27.7
11	91.8	9.3	75.7	25.6	75.5	26.1
12	91.0	9.7	75.3	25.6	75.7	29.9
13	90.5	10.2	72.3	28.6	75.4	38.2
14	89.6	11.7	73.4	26.3	75.7	37.4
15	88.7	12.5	74.7	25.3	75.3	40.2
16	86.1	14.3	64.3	37.4	75.7	42.4
17	86.3	16.3	66.3	34.7	75.2	40.2

Table 4. Performance comparison of UAD modules appended to different Stage 3 blocks. Results include accuracy (Acc) and equal error rate (EER) for FF++ (digital: deepfake, face2face and faceswap), SiW-Mv2 (physical: replay and print), and MSU-MFSD (physical: replay and print) datasets.

in Table 4. FF++ includes attack types such as digital Deepfake, Face2Face, and FaceSwap, while SiW-Mv2 and MSU-MFSD includes Physical Replay and Print attacks. Among all intermediate blocks, the sixth block of Stage 3 (i.e., Stage 3 Block 5) demonstrated the best performance across the evaluated datasets, making it most suitable for UAD tasks. This block extracts features that effectively balance low-frequency abstract representations with high-frequency texture-level details, which is crucial for joint attack detection, as it requires both broader structural inconsistencies and subtle local artifacts, which are key indicators of spoofing attempts. Therefore the results from the UAD module appended at the sixth block of Stage 3 (i.e., Stage 3 Block 5) are used as performance metrics for further analysis in this study. Additionally, since the backbone weights remain unchanged, the performance of FRM remain unaffected.

For digital spoof detection, our model achieved accuracies of 97.2% on the FF++, surpassing the performance over state-of-the-art deepfake detectors listed in Table 5. Also, for physical spoof detection, our model achieved 86.8% accuracy on SiW-Mv2, surpassing most state-of-the-art physical spoof detectors as illustrated in Table 6. These results confirms *equivalent* performance of our unified model for physical and digital attack detection over SOTA physical and digital (deepfake) attack detector baselines. The results highlights that UAD performs better when appended to intermediate blocks, as these blocks focus more on low-level features essential for joint physical-digital attack, over UAD head appended at the end of the Swin Transformer backbone.

Study	Model	Accuracy (%)
Chollet et al. (2017) [9]	Xception	74.1
Liu et al. (2021) [33]	Seferbekov	73.5
Wang et al. (2019) [5]	Eff.B1 + LSTM	68.3
Cozzolino et al. (2021) [10]	ID-Reveal	81.7
Zakkam et al. (2025) [59]	CoDeiT-XL	88.1
<b>Ours (Unified Approach)</b>	<b>UAD</b>	<b>97.2</b>

Table 5. Comparing performance of our model with state-of-the-art deepfake detectors evaluated on the FF++ dataset.

Study	Model	Accuracy (%)
Arora et al. (2021) [3]	Autoencoders	60.11
Deb and Jain (2021) [12]	SSR-FCN	80.1
Niraj et al. (2023) [52]	Mobilenet/PAD-CNN	92.0/89.0
Yu et al. (2020) [58]	CDCN	81.7
<b>Ours (Unified Approach)</b>	<b>UAD</b>	<b>86.8</b>

Table 6. Comparison of our model’s performance with state-of-the-art physical spoof detectors.

Additionally, we evaluated our unified model on unknown physical and digital spoofing attacks from the SiW-Mv2 and DFFD datasets, respectively. Table 7 and Table 8 demonstrate the results of our UAD model on unknown attacks, with the UAD module appended at 5<sup>th</sup> block of Stage 3. As can be seen from Table 7, the UAD module also obtains acceptable performance on unknown physical attacks with an average accuracy of 80.11%, with the highest being 98.12% for Mask Papermask and the lowest being 59.06% for Partial Paperglasses. The high accuracy of Mask Papermask is due to its distinct texture and structural artifacts, such as sharp edges and material-specific features, which are easily detected. In contrast, the lower accuracy for Partial Paperglasses stems from its minimal and localized changes, often confined to small regions like the eyes or glasses, making detection more challenging. Notably, the performance of our UAD on unknown physical attacks exceeds that reported in [2] for all types of Makeup attacks. While the accuracy for Makeup spoofing in [2] was 61.73%, our model achieves high accuracy of 74.23%, 72.45%, and 89.73% for Makeup Cosmetics, Makeup Impersonation, and Makeup Obfuscation spoof types, respectively. Furthermore, the accuracy of our unified model on unknown attacks namely Silicone, Partial Mouth, Partial Eye, and Mask Halfmask—categories not addressed in [2]—are 93.56%, 90.05%, 81.17%, and 80.91%, respectively.

As shown in Table 8, our UAD module achieves an average accuracy of **72.36%** on unknown digital attacks which are attribute manipulation based deepfakes from DFFD [11] dataset. Notably, the performance of our model is at par with the results reported in [35, 36] on unknown digital attacks, highlighting its effectiveness to unknown digital at-

SN	Spoof Type	Accuracy (%)
1	Makeup Cosmetics	74.23
2	Makeup Impersonation	72.45
3	Makeup Obfuscation	89.73
4	Mannequin	87.43
5	Mask Halfmask	80.91
6	<b>Mask Papermask</b>	<b>98.12</b>
7	Mask Transparent Mask	73.76
8	Partial Eye	81.17
9	Partial Funnyeyeglasses	60.91
10	Partial Mouth	90.05
11	Partial Paperglasses	59.06
12	Silicone	93.56

Table 7. Performance of UAD module appended at an intermediate block (Stage 3, Block 5) of the Swin Transformer backbone on unknown physical attacks from the SiW-Mv2 dataset.

SN	Spoof Type	Accuracy (%)
1	Faceapp	69.93
2	PGGAN_V1	74.70
3	PGGAN_V2	72.08
4	<b>StarGAN</b>	<b>77.34</b>
5	StyleGAN_CelebA	70.89
6	StyleGAN_FFHQ	69.27

Table 8. Performance of UAD module appended at an intermediate block (Stage 3, Block 5) of the Swin Transformer backbone on unknown digital attacks based on attribute manipulation from the DFFD dataset.

tacks.

These experiments highlight the efficacy of our proposed unified model in obtaining performance at par with the SOTA individual face recognition and physical and digital spoof detectors across datasets and unknown attack types.

## 6. Conclusion and Future Works

We proposed a unified model to jointly perform the physical-digital face attack detection and face-matching tasks. We exploit Swin Transformer architecture and leverage the local features extracted from the intermediate blocks in conjunction with HiLo attention and CNN for joint spoof detection while using the global features learned by the final layer for face matching. Experiments conducted in various settings demonstrate that our proposed unified model can achieve equivalent performance for both physical-digital attack detection and face-matching tasks in comparison to SOTA models across datasets and attack types. As a part of future work, we will evaluate the efficacy of our proposed unified model across different biometrics modalities and novel attack types based on different generation techniques.



## References

- [1] Kyeongjin Ahn, Seungeon Lee, Sungwon Han, Cheng Yaw Low, and Meeyoung Cha. Uncertainty-aware face embedding with contrastive learning for open-set evaluation. *IEEE Transactions on Information Forensics and Security*, 2024. [3](#)
- [2] Rouqaiyah Al-Refai and Karthik Nandakumar. A unified model for face matching and presentation attack detection using an ensemble of vision transformer features. In *Proceedings of the IEEE/CVF Winter Conference on Applications of Computer Vision*, pages 662–671, 2023. [2](#), [3](#), [6](#), [7](#), [8](#)
- [3] Shefali Arora, MPS Bhatia, and Vipul Mittal. A robust framework for spoofing detection in faces using deep learning. *The Visual Computer*, 38(7):2461–2472, 2022. [8](#)
- [4] Peter N. Belhumeur, Joao P Hespanha, and David J. Kriegman. Eigenfaces vs. fisherfaces: Recognition using class specific linear projection. *IEEE Transactions on pattern analysis and machine intelligence*, 19(7):711–720, 1997. [3](#)
- [5] Ksenia Bittner, Peter Reinartz, and Marco Korner. Late or earlier information fusion from depth and spectral data? large-scale digital surface model refinement by hybrid-cgan. In *Proceedings of the IEEE/CVF Conference on Computer Vision and Pattern Recognition (CVPR) Workshops*, June 2019. [8](#)
- [6] Zhimin Cao, Qi Yin, Xiaou Tang, and Jian Sun. Face recognition with learning-based descriptor. In *2010 IEEE Computer society conference on computer vision and pattern recognition*, pages 2707–2714. IEEE, 2010. [3](#)
- [7] Nicholas Carlini and David Wagner. Adversarial examples are not easily detected: Bypassing ten detection methods. In *Proceedings of the 10th ACM workshop on artificial intelligence and security*, pages 3–14, 2017. [2](#)
- [8] Yunjey Choi, Minje Choi, Munyoung Kim, Jung-Woo Ha, Sunghun Kim, and Jaegul Choo. Stargan: Unified generative adversarial networks for multi-domain image-to-image translation. In *Proceedings of the IEEE conference on computer vision and pattern recognition*, pages 8789–8797, 2018. [1](#)
- [9] François Chollet. Xception: Deep learning with depthwise separable convolutions. In *Proceedings of the IEEE conference on computer vision and pattern recognition*, pages 1251–1258, 2017. [8](#)
- [10] Davide Cozzolino, Andreas Rössler, Justus Thies, Matthias Nießner, and Luisa Verdoliva. Id-reveal: Identity-aware deepfake video detection. In *Proceedings of the IEEE/CVF international conference on computer vision*, pages 15108–15117, 2021. [8](#)
- [11] Hao Dang, Feng Liu, Joel Stehouwer, Xiaoming Liu, and Anil K Jain. On the detection of digital face manipulation. In *Proceedings of the IEEE/CVF Conference on Computer Vision and Pattern Recognition*, pages 5781–5790, 2020. [6](#), [8](#)
- [12] Debayan Deb and Anil K Jain. Look locally infer globally: A generalizable face anti-spoofing approach. *IEEE Transactions on Information Forensics and Security*, 16:1143–1157, 2020. [8](#)
- [13] Jiankang Deng, Jia Guo, Niannan Xue, and Stefanos Zafeiriou. Arcface: Additive angular margin loss for deep face recognition. In *Proceedings of the IEEE/CVF conference on computer vision and pattern recognition*, pages 4690–4699, 2019. [5](#), [6](#), [7](#)
- [14] Hao Fang, Ajian Liu, Jun Wan, Sergio Escalera, Chenxu Zhao, Xu Zhang, Stan Z Li, and Zhen Lei. Surveillance face anti-spoofing. *IEEE Transactions on Information Forensics and Security*, 2023. [1](#)
- [15] Hao Fang, Ajian Liu, Haocheng Yuan, Junze Zheng, Dingheng Zeng, Yanhong Liu, Jiankang Deng, Sergio Escalera, Xiaoming Liu, Jun Wan, et al. Unified physical-digital face attack detection. *arXiv preprint arXiv:2401.17699*, 2024. [2](#), [5](#), [6](#)
- [16] Xiao Guo, Yaojie Liu, Anil Jain, and Xiaoming Liu. Multi-domain learning for updating face anti-spoofing models. In *European Conference on Computer Vision*, pages 230–249. Springer, 2022. [5](#)
- [17] Xianhua He, Dashuang Liang, Song Yang, Zhanlong Hao, Hui Ma, Binjie Mao, Xi Li, Yao Wang, Pengfei Yan, and Ajian Liu. Joint physical-digital facial attack detection via simulating spoofing clues. In *Proceedings of the IEEE/CVF Conference on Computer Vision and Pattern Recognition*, pages 995–1004, 2024. [4](#)
- [18] Zhenliang He, Wangmeng Zuo, Meina Kan, Shiguang Shan, and Xilin Chen. Attgan: Facial attribute editing by only changing what you want. *IEEE transactions on image processing*, 28(11):5464–5478, 2019. [1](#)
- [19] Gee-Sern Jison Hsu, Jie-Ying Zhang, Huang Yu Hsiang, and Wei-Jie Hong. Pose adapted shape learning for large-pose face reenactment. In *Proceedings of the IEEE/CVF Conference on Computer Vision and Pattern Recognition*, pages 7413–7422, 2024. [3](#)
- [20] Sandy Huang, Nicolas Papernot, Ian Goodfellow, Yan Duan, and Pieter Abbeel. Adversarial attacks on neural network policies. *arXiv preprint arXiv:1702.02284*, 2017. [2](#)
- [21] Anil K Jain and Stan Z Li. *Handbook of face recognition*, volume 1. Springer, 2011. [1](#), [2](#)
- [22] Shan Jia, Guodong Guo, and Zhengquan Xu. A survey on 3d mask presentation attack detection and countermeasures. *Pattern recognition*, 98:107032, 2020. [1](#)
- [23] Arman Kereshe and Pakizar Shamoi. Liveness detection in computer vision: Transformer-based self-supervised learning for face anti-spoofing. *arXiv preprint arXiv:2406.13860*, 2024. [2](#)
- [24] Yuezun Li, Xin Yang, Pu Sun, Honggang Qi, and Siwei Lyu. Celeb-df: A large-scale challenging dataset for deepfake forensics. In *Proceedings of the IEEE/CVF conference on computer vision and pattern recognition*, pages 3207–3216, 2020. [5](#)
- [25] Li Lin, Irene Amerini, Xin Wang, Shu Hu, et al. Robust clip-based detector for exposing diffusion model-generated images. *arXiv preprint arXiv:2404.12908*, 2024. [2](#)
- [26] Ajian Liu, Xuan Li, Jun Wan, Yanyan Liang, Sergio Escalera, Hugo Jair Escalante, Meysam Madadi, Yi Jin, Zhuoyuan Wu, Xiaogang Yu, et al. Cross-ethnicity face anti-spoofing recognition challenge: A review. *IET Biometrics*, 10(1):24–43, 2021. [1](#), [2](#)

- [27] Ajian Liu, Zichang Tan, Jun Wan, Sergio Escalera, Guodong Guo, and Stan Z Li. Casia-surf cefa: A benchmark for multi-modal cross-ethnicity face anti-spoofing. In *Proceedings of the IEEE/CVF winter conference on applications of computer vision*, pages 1179–1187, 2021. [1](#)
- [28] Ajian Liu, Jun Wan, Sergio Escalera, Hugo Jair Escalante, Zichang Tan, Qi Yuan, Kai Wang, Chi Lin, Guodong Guo, Isabelle Guyon, et al. Multi-modal face anti-spoofing attack detection challenge at cvpr2019. In *Proceedings of the IEEE CVPRW*, pages 0–0, 2019. [1](#), [2](#)
- [29] Ajian Liu, Chenxu Zhao, Zitong Yu, Anyang Su, Xing Liu, Zijian Kong, Jun Wan, Sergio Escalera, Hugo Jair Escalante, Zhen Lei, et al. 3d high-fidelity mask face presentation attack detection challenge. In *Proceedings of the IEEE/CVF international conference on computer vision*, pages 814–823, 2021. [1](#)
- [30] Ajian Liu, Chenxu Zhao, Zitong Yu, Jun Wan, Anyang Su, Xing Liu, Zichang Tan, Sergio Escalera, Junliang Xing, Yanyan Liang, et al. Contrastive context-aware learning for 3d high-fidelity mask face presentation attack detection. *IEEE Transactions on Information Forensics and Security*, 17:2497–2507, 2022.
- [31] Chengjun Liu and Harry Wechsler. Gabor feature based classification using the enhanced fisher linear discriminant model for face recognition. *IEEE Transactions on Image processing*, 11(4):467–476, 2002. [3](#)
- [32] Shuhua Liu, Yu Song, Mengyu Zhang, Jianwei Zhao, Shihao Yang, and Kun Hou. An identity authentication method combining liveness detection and face recognition. *Sensors*, 19(21):4733, 2019. [3](#)
- [33] Zhaoyang Liu, Yutong Lin, Yue Cao, Han Hu, Yixuan Wei, Zheng Zhang, Stephen Lin, and Baining Guo. Proceedings of the ieeecvfi international conference on computer vision. In *Proceedings of the IEEE/CVF International Conference on Computer Vision*, pages 10012–10022, 2021. [8](#)
- [34] Ze Liu, Yutong Lin, Yue Cao, Han Hu, Yixuan Wei, Zheng Zhang, Stephen Lin, and Baining Guo. Swin transformer: Hierarchical vision transformer using shifted windows. In *Proceedings of the IEEE/CVF international conference on computer vision*, pages 10012–10022, 2021. [1](#), [2](#), [3](#), [6](#)
- [35] Aakash Varma Nadimpalli and Ajita Rattani. Proactive deepfake detection using gan-based visible watermarking. *ACM Transactions on Multimedia Computing, Communications and Applications*, 20(11):1–27, 2024. [8](#)
- [36] Aakash Varma Nadimpalli and Ajita Rattani. Social media authentication and combating deepfakes using semi-fragile invisible image watermarking. *Digital Threats*, 5(4), Dec. 2024. [8](#)
- [37] Zizheng Pan, Jianfei Cai, and Bohan Zhuang. Fast vision transformers with hilo attention. *Advances in Neural Information Processing Systems*, 35:14541–14554, 2022. [2](#), [4](#)
- [38] Omkar Parkhi, Andrea Vedaldi, and Andrew Zisserman. Deep face recognition. In *BMVC 2015-Proceedings of the British Machine Vision Conference 2015*. British Machine Vision Association, 2015. [3](#)
- [39] Divyarajsinh N Parmar and Brijesh B Mehta. Face recognition methods & applications. *arXiv preprint arXiv:1403.0485*, 2014. [1](#)
- [40] Gan Pei, Jiangning Zhang, Menghan Hu, Zhenyu Zhang, Chengjie Wang, Yunsheng Wu, Guangtao Zhai, Jian Yang, Chunhua Shen, and Dacheng Tao. Deepfake generation and detection: A benchmark and survey. *arXiv preprint arXiv:2403.17881*, 2024. [2](#)
- [41] Gracile Astlin Pereira and Muhammad Hussain. A review of transformer-based models for computer vision tasks: Capturing global context and spatial relationships. *arXiv preprint arXiv:2408.15178*, 2024. [1](#)
- [42] Lixiong Qin, Mei Wang, Chao Deng, Ke Wang, Xi Chen, Jiani Hu, and Weihong Deng. Swinface: a multi-task transformer for face recognition, expression recognition, age estimation and attribute estimation. *IEEE Transactions on Circuits and Systems for Video Technology*, 2023. [3](#)
- [43] Rajeev Ranjan, Swami Sankaranarayanan, Ankan Bansal, Navaneeth Bodla, Jun-Cheng Chen, Vishal M Patel, Carlos D Castillo, and Rama Chellappa. Deep learning for understanding faces: Machines may be just as good, or better, than humans. *IEEE Signal Processing Magazine*, 35(1):66–83, 2018. [1](#)
- [44] Felix Rosberg, Eren Erdal Aksoy, Fernando Alonso-Fernandez, and Cristofer Englund. Facedancer: Pose-and occlusion-aware high fidelity face swapping. In *Proceedings of the IEEE/CVF winter conference on applications of computer vision*, pages 3454–3463, 2023. [1](#)
- [45] Andreas Rossler, Davide Cozzolino, Luisa Verdoliva, Christian Riess, Justus Thies, and Matthias Nießner. Faceforensics++: Learning to detect manipulated facial images. In *Proceedings of the IEEE/CVF international conference on computer vision*, pages 1–11, 2019. [5](#)
- [46] Florian Schroff, Dmitry Kalenichenko, and James Philbin. Facenet: A unified embedding for face recognition and clustering. In *Proceedings of the IEEE conference on computer vision and pattern recognition*, pages 815–823, 2015. [3](#)
- [47] ST Suganthi, Mohamed Uvaze Ahamed Ayoobkhan, Nebojsa Bacanin, K Venkatachalam, Hubálovský Štěpán, Trojovský Pavel, et al. Deep learning model for deep fake face recognition and detection. *PeerJ Computer Science*, 8:e881, 2022. [3](#)
- [48] Zhonglin Sun and Georgios Tzimiropoulos. Part-based face recognition with vision transformers. *arXiv preprint arXiv:2212.00057*, 2022. [3](#)
- [49] Yaniv Taigman, Ming Yang, Marc’Aurelio Ranzato, and Lior Wolf. Deepface: Closing the gap to human-level performance in face verification. In *Proceedings of the IEEE conference on computer vision and pattern recognition*, pages 1701–1708, 2014. [3](#)
- [50] Niloufar Alipour Talemi, Hossein Kashiani, and Nasser M Nasrabadi. Catface: Cross-attribute-guided transformer with self-attention distillation for low-quality face recognition. *IEEE Transactions on Biometrics, Behavior, and Identity Science*, 2024. [3](#)
- [51] Xiaoyang Tan, Yi Li, Jun Liu, and Lin Jiang. Face liveness detection from a single image with sparse low rank bilinear discriminative model. In *Computer Vision—ECCV 2010: 11th European Conference on Computer Vision, Heraklion, Crete, Greece, September 5–11, 2010, Proceedings, Part VI 11*, pages 504–517. Springer, 2010. [3](#)

- [52] Niraj Thapa, Meenal Chaudhari, and Kaushik Roy. Presentation attack detection: an analysis of spoofing in the wild (siw) dataset using deep learning models. *Discover Artificial Intelligence*, 3(1):30, 2023. 8
- [53] Mei Wang and Weihong Deng. Deep face recognition: A survey. *Neurocomputing*, 429:215–244, 2021. 1, 2
- [54] Kota Watanabe, Koichi Ito, and Takafumi Aoki. Spoofing attack detection in face recognition system using vision transformer with patch-wise data augmentation. In *2022 Asia-Pacific Signal and Information Processing Association Annual Summit and Conference (APSIPA ASC)*, pages 1561–1565. IEEE, 2022. 2
- [55] Di Wen, Hu Han, and Anil K Jain. Face spoof detection with image distortion analysis. *IEEE Transactions on Information Forensics and Security*, 10(4):746–761, 2015. 6
- [56] Yihang Wu. Quality network based on enhanced confidence-aware and adaptive margin for facial recognition. In *2024 4th International Conference on Machine Learning and Intelligent Systems Engineering (MLISE)*, pages 352–355. IEEE, 2024. 3
- [57] Dong Yi, Zhen Lei, Shengcai Liao, and Stan Z Li. Learning face representation from scratch. *arXiv preprint arXiv:1411.7923*, 2014. 5
- [58] Zitong Yu, Chenxu Zhao, Zezheng Wang, Yunxiao Qin, Zhuo Su, Xiaobai Li, Feng Zhou, and Guoying Zhao. Searching central difference convolutional networks for face anti-spoofing. In *Proceedings of the IEEE/CVF conference on computer vision and pattern recognition*, pages 5295–5305, 2020. 8
- [59] John Zakkam, Umarani Jayaraman, Subin Sahayam, and Ajita Rattani. Codeit: Contrastive data-efficient transformers for deepfake detection. In *International Conference on Pattern Recognition*, pages 62–77. Springer, 2025. 2, 8
- [60] Kaipeng Zhang, Zhanpeng Zhang, Zhifeng Li, and Yu Qiao. Joint face detection and alignment using multitask cascaded convolutional networks. *IEEE signal processing letters*, 23(10):1499–1503, 2016. 2, 6
- [61] Shifeng Zhang, Ajian Liu, Jun Wan, Yanyan Liang, Guodong Guo, Sergio Escalera, Hugo Jair Escalante, and Stan Z Li. Casia-surf: A large-scale multi-modal benchmark for face anti-spoofing. *IEEE Transactions on Biometrics, Behavior, and Identity Science*, 2(2):182–193, 2020. 1, 2
- [62] Shifeng Zhang, Xiaobo Wang, Ajian Liu, Chenxu Zhao, Jun Wan, Sergio Escalera, Hailin Shi, Zezheng Wang, and Stan Z Li. A dataset and benchmark for large-scale multi-modal face anti-spoofing. In *Proceedings of the IEEE/CVF Conference on Computer Vision and Pattern Recognition*, pages 919–928, 2019. 1, 2
- [63] Yaoyao Zhong and Weihong Deng. Face transformer for recognition. *arXiv preprint arXiv:2103.14803*, 2021. 2, 3